Research Article

Image Encryption Algorithm Using Differential Equations

Mohammed Abdul Hameed Jassim Al-Kufi1, Hamdy El-Metwally2, AbdelRahman Karawia3

1,2,3 Department of Mathematics, Faculty of Science, Mansoura University

1mohammeda.alkufi@uokufa.edu.iq, 2 helmetwally@mans.edu.eg, 3abibka@mans.edu.eg

ARTICLE INFO	ABSTRACT
	After several prior works in image encryption, where we utilized algebraic mathematical tools within matrix algebra to perform operations that scatter the color values of the image, transforming the image into an encrypted matrix that no longer represents the original image, we decided to explore the field of differential equations as a mathematical tool for image encryption. In this algorithm, we employed third-order ordinary differential equations along with first-degree equations to encode the image. We treated the color values of the original image as coefficients for the independent variable x. Then, we selected another image as an encryption key, considering its color values as the powers associated with the independent variable x. This process yielded a system of third-order differential equations, the number of which elements equaled the number of color values in the original image. We approached this system of differential equations by integrating with respect to the independent variable x three times for each system of differential equations obtained, treating the integration constant as zero. Ultimately, we obtained a system of ordinary equations with the independent variable x, where the coefficients of this variable represented alternative values for the color values of the original image. These coefficients represented a scattering of the color values of the original image, and the new matrix formed by these values represented the encryption matrix for the original image. For the purpose of decryption and recovering the original image, we referred to the key image used during the encryption process. We followed these steps: We took the numerical values of the encrypted matrix and converted them into coefficients for the independent variable x. We considered the color values of the key matrix as the powers associated with the independent variable x after adding 3 to them. This step yielded a system of ordinary equations with the number of elements corresponding to the number of color values in the original image. Subsequently, we differentiated each equation in the system of ordinary equations mentioned above. We repeated the differentiation process three times, ultimately obtaining a system of differential equations with the independent variable x, where the coefficients of this variable represented the color values of the image after decryption. These values matched the color values of the original image prior to decryption, confirming that the error value equaled zero. The results we obtained were excellent and matched high standards of accuracy, which we will discuss later. **Keywords:** Digital Image, Differential Equations, Integration, Differentiation, Encryption, Decryption.

INTRODUCTION

In this introduction, we will discuss the definitions of Differential and Integral Equations and then delve into the core of the algorithm and results.

A digital image is a numerical matrix with three bands, making it a three-dimensional matrix. Each band corresponds to a color (green, blue, and red) [1], [2]. The numerical values in each band represent the brightness intensity of each pixel in the image. We will not delve into pixel explanations here, but we will state that an image consists of a collection of small squares arranged in a regular pattern, where each square represents a single pixel. Each pixel has three colors that determine the brightness intensity of each color—the numerical value for that color in the corresponding band [3], [4]. This means that the pixel color is a mixture of three colors with different brightness intensities [5]. The brightness levels for each color range from 0 to 255, indicating that the possible number of colors for each pixel is 16,777,216. The color combinations of the pixels composing the image ultimately create a beautiful representation of a specific scene, face, or other subjects [6].

Furthermore, [7] underscores how deep learning enhances the efficiency and accuracy of 3D reconstruction by leveraging pixel data and algorithms to transform 2D images into dynamic 3D representations.

Digital images are divided into several formats. After capturing personal photos, we usually save image files in various formats, each with its own unique purpose. The most commonly used formats include TIFF, JPEG, PNG, and DNG, which are often found as default options in most DSLR digital cameras [7][8].

Some of these well-known extensions are as follows:

(RAW , DNG , TIFF , GIF , JPEG , BMP , PNG)[8]

The details of images are present only within a limited range. Hence, studying the structure of an image, describable through multiple-scale local derivatives of the image using contour lines and local coordinate systems, becomes crucial. We will also employ differential geometry tools, which are defined as a framework of finite-dimensional real manifolds, utilizing analytical methods to investigate geometrical problems, including the shapes of curves, smooth surfaces, lines, distances, surfaces, and so forth [9]. An important characteristic of real images is that they exist as structurally meaningful within specific scales. For example, the concept of a tree section is logical only on a scale ranging from a few centimeters to at most a few meters. Discussing the idea of a tree at the nanometer or kilometer level is meaningless. In these scales, it is appropriate to talk about the particles composing the leaves of the tree and the forest in which the tree grows, respectively. This is the reality – images manifest differently depending on the appropriate scale, as these scales have significant effects when one aims to describe them accurately [10]. It becomes evident that the concept of scale is of utmost importance when we consider that the theory of Hilbert space offers a mathematically convenient way to create representations of images with multiple scales, which also deals with what was mentioned earlier [11]. Nature itself is inherently multiscale in image data. The reason behind constructing each scale is that, if no prior information is available about what the suitable scales are for a given dataset, the only reasonable approach for a non-committed vision system is to represent the input visual data at multiple levels [12].

One can confidently declare that differential equations represent the most profound and widely used class of mathematical tools for the description of almost all engineering, mathematical, and scientific problems. They are particularly useful in the modeling of systems such as heat transfer, fluid dynamics, wave propagation, electronic circuits, as well as structural analysis and chemical reaction kinetics [13]. In algebraic terms, differential equations can be defined as equations that have derivatives or differentials of some definite functions involved, with the variables of these derivatives being dependent on them. The main goal in solving these equations is to find the mathematical functions that meet the specified derivatives [13].

Moreover, Hutaihit, Hammed, and Shauchuk [14] emphasize the importance of geometrical descriptors in analyzing complex systems. Their work highlights how the identification of lines based on form factors can enhance the understanding and solution of differential equations in various engineering applications, thus integrating geometric considerations into mathematical modeling.

 In a general sense, a differential equation in the realm of mathematics can be said to involve the variable being a function and the relationship established between the function and its derivatives. The process of solving such an equation would require determining all functions y that satisfy it, and these functions together make up the general solution or solution family for that particular equation. Every single function belonging to this collection is known as a particular solution of the equation [14].

On the other hand, a regular differential equation (ODE) describes a function of only one variable, whereas a partial differential equation (PDE) pertains to a function that has multiple variables with its derivatives also being partial derivatives [15].

Differential equations are very important for explaining scientific phenomena in physics and chemistry. This is because you can create equations using multiple variables as differential functions, such as the speed and position of various objects. Therefore, it is important to know how to solve these equations and how to process them. Note that it is often impossible to solve equations completely algebraically. Therefore, it is important to have a good understanding of the theory and properties of these equations, which naturally facilitates the formulation of solutions [16].

Differential and Integral Equations

Equations can be classified according to their order, which is defined by the largest derivative included in the equation. The degree of the equation is proportional to the exponent to which the greatest derivative is raised [17][18].

We'll suffice with what we've covered about differential equations, and we don't intend to delve deeper into this topic because, in our current research, it serves merely as a tool for performing color value dispersion of the image for the purpose of encryption. This is what we will explain later in the course of our research.

Encryption

Definition of Encryption:

In the field of cybersecurity, encryption is the critical process of changing data from a readable format to an encrypted form, rendering it indecipherable until decoded [19][20]. Encryption, as a cornerstone of data security, is the most fundamental and critical technology for protecting information from unauthorized access or theft, defeating any malicious efforts to exploit it [21][22]. Encryption, which is widely used by both

individual users and huge organizations, protects transmitted information, ranging from sensitive payment data to personal details, when it is shared between web browsers and servers [21][22]. Encryption software, often known as "encryption algorithms" or simply "encryption," allows for the design of encryption protocols that are theoretically resistant to decryption in the absence of significant processing resources [23][24].

1. Methodology:

The mathematical tool used in our algorithm is ordinary third-order differential equations, and we will explain the encryption and decryption process through a practical example before delving into the results, readings, and comparisons.

Methodology of proposed algorithm of encryption and decryption:

2.1   Practical example: -

We have two hypothetical matrices representing the image we want to encrypt and the key image, as follows:

Let the matrix of origon image $A_{(3,6)} = \begin{bmatrix} 215 & 145 & 111 & 145 & 123 & 245 \\ 221 & 159 & 170 & 251 & 154 & 201 \\ 200 & 233 & 177 & 101 & 143 & 125 \end{bmatrix}$

Let the matrix of key image $B_{(3,6)} = \begin{bmatrix} 128 & 222 & 98 & 76 & 114 & 246 \\ 28 & 222 & 178 & 66 & 99 & 109 \\ 254 & 178 & 244 & 118 & 243 & 225 \end{bmatrix}$

First: Encryption

The system of differential equations of the third order generated from the two matrices $A_{(3,6)}$ and $B_{(3,6)}$ and let it be $C_{(3,6)}$.

$C_{(3,6)} =$
$$\begin{bmatrix} y'''_{(1,1)} = 215x^{128} & y'''_{(1,2)} = 145x^{222} & y'''_{(1,3)} = 111x^{98} & y'''_{(1,4)} = 145x^{76} & y'''_{(1,5)} = 123x^{114} & y'''_{(1,6)} = 245x^{246} \\ y'''_{(2,1)} = 221x^{28} & y'''_{(2,2)} = 159x^{222} & y'''_{(2,3)} = 170x^{178} & y'''_{(2,4)} = 251x^{66} & y'''_{(2,5)} = 154x^{99} & y'''_{(2,6)} = 201x^{109} \\ y'''_{(3,1)} = 200x^{254} & y'''_{(3,2)} = 233x^{178} & y'''_{(3,3)} = 177x^{244} & y'''_{(3,4)} = 101x^{118} & y'''_{(3,5)} = 143x^{243} & y'''_{(3,6)} = 125x^{225} \end{bmatrix}$$

This matrix of third-order differential equations will be the basis for the encryption process we desire. The dispersion of color values will occur in three stages because the first and second stages are not sufficient to conceal the image's features, as follows:

Step One: We perform a first-order integration operation for all the differential equations in the system $C_{(3,6)}$, and we will name the resulting matrix $D1_{(3,6)}$

$D1_{(3,6)}$
$$= \begin{bmatrix} y''_{(1,1)} = \frac{215}{129}x^{129} + c1_{(1,1)} & y''_{(1,2)} = \frac{145}{223}x^{223} + c1_{(1,2)} & y''_{(1,3)} = \frac{111}{99}x^{99} + c1_{(1,3)} & y''_{(1,4)} = \frac{145}{77}x^{77} + c1_{(1,4)} & y''_{(1,5)} = \frac{123}{115}x^{115} + c1_{(1,5)} & y''_{(1,6)} = \frac{245}{247}x^{247} + c1_{(1,6)} \\ y''_{(2,1)} = \frac{221}{29}x^{29} + c1_{(2,1)} & y''_{(2,2)} = \frac{159}{223}x^{223} + c1_{(2,2)} & y''_{(2,3)} = \frac{170}{179}x^{179} + c1_{(2,3)} & y''_{(2,4)} = \frac{251}{67}x^{67} + c1_{(2,4)} & y''_{(2,5)} = \frac{154}{100}x^{100} + c1_{(2,5)} & y''_{(2,6)} = \frac{201}{110}x^{110} + c1_{(2,6)} \\ y''_{(3,1)} = \frac{200}{255}x^{255} + c1_{(3,1)} & y''_{(3,2)} = \frac{233}{179}x^{179} + c1_{(3,2)} & y''_{(3,3)} = \frac{177}{245}x^{245} + c1_{(3,3)} & y''_{(3,4)} = \frac{101}{119}x^{119} + c1_{(3,4)} & y''_{(3,5)} = \frac{143}{244}x^{244} + c1_{(3,5)} & y''_{(3,6)} = \frac{125}{226}x^{226} + c1_{(3,6)} \end{bmatrix}$$

This matrix represents a second-order system of differential equations with integration constants $c1_{(i,j)}$ $i = 1 \dots 3$ and $j = 1, 2, \dots, 6$ As a special case, we will consider all integration constants to be zero. Thus, the matrix for the second-order system of differential equations is as follows:

$D1_{(3,6)}$
$$= \begin{bmatrix} y''_{(1,1)} = \frac{215}{129}x^{129} & y''_{(1,2)} = \frac{145}{223}x^{223} & y''_{(1,3)} = \frac{111}{99}x^{99} & y''_{(1,4)} = \frac{145}{77}x^{77} & y''_{(1,5)} = \frac{123}{115}x^{115} & y''_{(1,6)} = \frac{245}{247}x^{247} \\ y''_{(2,1)} = \frac{221}{29}x^{29} & y''_{(2,2)} = \frac{159}{223}x^{223} & y''_{(2,3)} = \frac{170}{179}x^{179} & y''_{(2,4)} = \frac{251}{67}x^{67} & y''_{(2,5)} = \frac{154}{100}x^{100} & y''_{(2,6)} = \frac{201}{110}x^{110} \\ y''_{(3,1)} = \frac{200}{255}x^{255} & y''_{(3,2)} = \frac{233}{179}x^{179} & y''_{(3,3)} = \frac{177}{245}x^{245} & y''_{(3,4)} = \frac{101}{119}x^{119} & y''_{(3,5)} = \frac{143}{244}x^{244} & y''_{(3,6)} = \frac{125}{226}x^{226} \end{bmatrix}$$

From the above system of second-order differential equations, we derive the first dispersion process for the color values of the original image. This process involves the coefficients of the independent variable x, as follows:

$$SCRAMBLE1_{(3,6)} = \begin{bmatrix} \overline{215} & \overline{145} & \overline{111} & \overline{145} & \overline{123} & \overline{245} \\ \overline{129} & \overline{223} & \overline{99} & \overline{77} & \overline{115} & \overline{247} \\ 221 & 159 & 170 & 251 & 154 & 201 \\ \overline{29} & \overline{223} & \overline{179} & \overline{67} & \overline{100} & \overline{110} \\ 200 & 233 & 177 & 101 & 143 & 125 \\ \overline{255} & \overline{179} & \overline{245} & \overline{119} & \overline{244} & \overline{226} \end{bmatrix}$$

The matrix **SCRAMBLE1$_{(3,6)}$** represents the initial dispersion of color values for the original image, which is a weak dispersion since the resulting image resembles the original one. Therefore, we proceed to the second step in the algorithm.

Step Two: We perform a second integration process for each differential equation in the system $D_{1(3,6)}$ and we will refer to the resulting matrix as $D_{2(3,6)}$

$D_{2(3,6)}$

$$= \begin{bmatrix} y'_{(1,1)} = \frac{\frac{215}{129}}{130}x^{130} \\ +c2_{(1,1)} \end{bmatrix} \quad \begin{matrix} y'_{(1,2)} = \frac{\frac{145}{223}}{224}x^{224} \\ +c2_{(1,2)} \end{matrix} \quad \begin{matrix} y'_{(1,3)} = \frac{\frac{111}{99}}{100}x^{100} \\ +c2_{(1,3)} \end{matrix} \quad \begin{matrix} y'_{(1,4)} = \frac{\frac{145}{77}}{78}x^{78} \\ +c2_{(1,4)} \end{matrix} \quad \begin{matrix} y'_{(1,5)} = \frac{\frac{123}{115}}{116}x^{116} \\ +c2_{(1,5)} \end{matrix} \quad \begin{matrix} y'_{(1,6)} = \frac{\frac{245}{247}}{248}x^{248} \\ +c2_{(1,6)} \end{matrix}$$

with rows:

$$y'_{(2,1)} = \frac{\frac{221}{29}}{30}x^{30}+c2_{(2,1)} \quad y'_{(2,2)} = \frac{\frac{159}{223}}{224}x^{224}+c2_{(2,2)} \quad y'_{(2,3)} = \frac{\frac{170}{179}}{180}x^{180}+c2_{(2,3)} \quad y'_{(2,4)} = \frac{\frac{251}{67}}{68}x^{68}+c2_{(2,4)} \quad y'_{(2,5)} = \frac{\frac{154}{100}}{101}x^{101}+c2_{(2,5)} \quad y'_{(2,6)} = \frac{\frac{201}{110}}{111}x^{111}+c2_{(2,6)}$$

$$y'_{(3,1)} = \frac{\frac{200}{255}}{256}x^{256}+c2_{(3,1)} \quad y'_{(3,2)} = \frac{\frac{233}{179}}{180}x^{180}+c2_{(3,2)} \quad y'_{(3,3)} = \frac{\frac{177}{245}}{246}x^{246}+c2_{(3,3)} \quad y'_{(3,4)} = \frac{\frac{101}{119}}{120}x^{120}+c2_{(3,4)} \quad y'_{(3,5)} = \frac{\frac{143}{244}}{245}x^{245}+c2_{(3,5)} \quad y'_{(3,6)} = \frac{\frac{125}{226}}{227}x^{227}+c2_{(3,6)}$$

This is a matrix of a first-order system of differential equations, with integration constants $c2_{(i,j)}$ $i = 1\ldots3$ $and\ j = 1,2,\ldots,6$. As a special case, we consider all integration constants to be zero. Therefore, the matrix of the first-order system of differential equations is as follows:

$D_{2(3,6)}$

$$= \begin{bmatrix} y'_{(1,1)} = \frac{\frac{215}{129}}{130}x^{130} & y'_{(1,2)} = \frac{\frac{145}{223}}{224}x^{224} & y'_{(1,3)} = \frac{\frac{111}{99}}{100}x^{100} & y'_{(1,4)} = \frac{\frac{145}{77}}{78}x^{78} & y'_{(1,5)} = \frac{\frac{123}{115}}{116}x^{116} & y'_{(1,6)} = \frac{\frac{245}{247}}{248}x^{248} \\ y'_{(2,1)} = \frac{\frac{221}{29}}{30}x^{30} & y'_{(2,2)} = \frac{\frac{159}{223}}{224}x^{224} & y'_{(2,3)} = \frac{\frac{170}{179}}{180}x^{180} & y'_{(2,4)} = \frac{\frac{251}{67}}{68}x^{68} & y'_{(2,5)} = \frac{\frac{154}{100}}{101}x^{101} & y'_{(2,6)} = \frac{\frac{201}{110}}{111}x^{111} \\ y'_{(3,1)} = \frac{\frac{200}{255}}{256}x^{256} & y'_{(3,2)} = \frac{\frac{233}{179}}{180}x^{180} & y'_{(3,3)} = \frac{\frac{177}{245}}{246}x^{246} & y'_{(3,4)} = \frac{\frac{101}{119}}{120}x^{120} & y'_{(3,5)} = \frac{\frac{143}{244}}{245}x^{245} & y'_{(3,6)} = \frac{\frac{125}{226}}{227}x^{227} \end{bmatrix}$$

From the above system of first-order differential equations, we obtain the second dispersion process for the color values of the original image. This process involves the coefficients of the independent variable x as follows:

$$SCRAMBLE2_{(3,6)} = \begin{bmatrix} \overline{215} & \overline{145} & \overline{111} & \overline{145} & \overline{123} & \overline{245} \\ \overline{129} & \overline{223} & \overline{99} & \overline{77} & \overline{115} & \overline{247} \\ 130 & 224 & 100 & 78 & 116 & 248 \\ 221 & 159 & 170 & 251 & 154 & 201 \\ \overline{29} & \overline{223} & \overline{179} & \overline{67} & \overline{100} & \overline{110} \\ 30 & 224 & 180 & 68 & 101 & 111 \\ 200 & 233 & 177 & 101 & 143 & 125 \\ \overline{255} & \overline{179} & \overline{245} & \overline{119} & \overline{244} & \overline{226} \\ 256 & 180 & 246 & 120 & 245 & 227 \end{bmatrix}$$

The matrix **SCRAMBLE2$_{(3,6)}$** represents a second-level dispersion for the color values of the original image. This is also a weak dispersion as the resulting image still resembles the original image. Therefore, we proceed to the third step in the algorithm.

Step Three: We perform a third integration operation for each of the differential equations in the system $D_{2(3,6)}$, and we will name the resulting matrix $D_{3(3,6)}$

$D_{3(3,6)}$

$$= \begin{bmatrix}
y_{(1,1)} = \dfrac{\frac{215}{129}}{\frac{130}{131}}x^{131} & y_{(1,2)} = \dfrac{\frac{145}{223}}{\frac{224}{225}}x^{225} & y_{(1,3)} = \dfrac{\frac{111}{99}}{\frac{100}{101}}x^{101} & y_{(1,4)} = \dfrac{\frac{145}{77}}{\frac{78}{79}}x^{79} & y_{(1,5)} = \dfrac{\frac{123}{115}}{\frac{116}{117}}x^{117} & y_{(1,6)} = \dfrac{\frac{245}{247}}{\frac{248}{249}}x^{249} \\
\quad +c3_{(1,1)} & \quad +c3_{(1,2)} & \quad +c3_{(1,3)} & \quad +c3_{(1,4)} & \quad +c3_{(1,5)} & \quad +c3_{(1,6)} \\[2mm]
y_{(2,1)} = \dfrac{\frac{221}{29}}{\frac{30}{31}}x^{31} & y_{(2,2)} = \dfrac{\frac{159}{223}}{\frac{224}{225}}x^{225} & y_{(2,3)} = \dfrac{\frac{170}{179}}{\frac{180}{181}}x^{181} & y_{(2,4)} = \dfrac{\frac{251}{67}}{\frac{68}{69}}x^{69} & y_{(2,5)} = \dfrac{\frac{154}{100}}{\frac{101}{102}}x^{102} & y_{(2,6)} = \dfrac{\frac{201}{110}}{\frac{111}{112}}x^{112} \\
\quad +c3_{(2,1)} & \quad +c3_{(2,2)} & \quad +c3_{(2,3)} & \quad +c3_{(2,4)} & \quad +c3_{(2,5)} & \quad +c3_{(2,6)} \\[2mm]
y_{(3,1)} = \dfrac{\frac{200}{255}}{\frac{256}{257}}x^{257} & y_{(3,2)} = \dfrac{\frac{233}{179}}{\frac{180}{181}}x^{181} & y_{(3,3)} = \dfrac{\frac{177}{245}}{\frac{246}{247}}x^{247} & y_{(3,4)} = \dfrac{\frac{101}{119}}{\frac{120}{121}}x^{121} & y_{(3,5)} = \dfrac{\frac{143}{244}}{\frac{245}{246}}x^{246} & y_{(3,6)} = \dfrac{\frac{125}{226}}{\frac{227}{228}}x^{228} \\
\quad +c3_{(3,1)} & \quad +c3_{(3,2)} & \quad +c3_{(3,3)} & \quad +c3_{(3,4)} & \quad +c3_{(3,5)} & \quad +c3_{(3,6)}
\end{bmatrix}$$

This is a matrix of the ordinary differential equations system with integration constants $c3_{(i,j)}$ $i = 1 \ldots 3$ $and\ j = 1, 2, \ldots, 6$. At this stage, if we examine the third dispersion of color values for the original image, which consists of coefficients of the independent variable x in the last matrix of the ordinary differential equations system, it will be as follows:

$$SCRAMBLE3_{(3,6)} = \begin{bmatrix}
\frac{215}{129} & \frac{145}{223} & \frac{111}{99} & \frac{145}{77} & \frac{123}{115} & \frac{245}{247} \\
\frac{130}{131} & \frac{224}{225} & \frac{100}{101} & \frac{78}{79} & \frac{116}{117} & \frac{248}{249} \\
221 & 159 & 170 & 251 & 154 & 201 \\
\frac{29}{30} & \frac{223}{224} & \frac{179}{180} & \frac{67}{68} & \frac{100}{101} & \frac{110}{111} \\
31 & 225 & 181 & 69 & 102 & 112 \\
200 & 233 & 177 & 101 & 143 & 125 \\
\frac{255}{256} & \frac{179}{180} & \frac{245}{246} & \frac{119}{120} & \frac{244}{245} & \frac{226}{227} \\
257 & 181 & 247 & 121 & 246 & 228
\end{bmatrix}$$

If we have found sufficient dispersion that leads to complete concealment of the image, we leave the integration constants $c3_{(i,j)}$ $i = 1 \ldots 3$ $and\ j = 1, 2, \ldots, 6$ in the matrix of the ordinary differential equations system in their general form. Because essentially, we will take the matrix related to the coefficients of the independent variable x present in the last matrix of the ordinary differential equations system, **SCRAMBLE3(3,6),** which represents the complete encryption of the original image.

Through the practical explanation using an example from the images that will be provided later, we will see how **SCRAMBLE1(3,6)** and **SCRAMBLE2(3,6)** represent a weak encryption of the image, and that **SCRAMBLE3(3,6)** is the complete encryption of the image.

Second: Decryption

We have the encrypted image matrix.

$$\text{encrypted image:} - SCRAMBLE3_{(3,6)} = \begin{bmatrix}
\frac{215}{129} & \frac{145}{223} & \frac{111}{99} & \frac{145}{77} & \frac{123}{115} & \frac{245}{247} \\
\frac{130}{131} & \frac{224}{225} & \frac{100}{101} & \frac{78}{79} & \frac{116}{117} & \frac{248}{249} \\
221 & 159 & 170 & 251 & 154 & 201 \\
\frac{29}{30} & \frac{223}{224} & \frac{179}{180} & \frac{67}{68} & \frac{100}{101} & \frac{110}{111} \\
31 & 225 & 181 & 69 & 102 & 112 \\
200 & 233 & 177 & 101 & 143 & 125 \\
\frac{255}{256} & \frac{179}{180} & \frac{245}{246} & \frac{119}{120} & \frac{244}{245} & \frac{226}{227} \\
257 & 181 & 247 & 121 & 246 & 228
\end{bmatrix}$$

Similarly, we have the key image matrix.

$$B_{(3,6)} = \begin{bmatrix}
128 & 222 & 98 & 76 & 114 & 246 \\
28 & 222 & 178 & 66 & 99 & 109 \\
254 & 178 & 244 & 118 & 243 & 225
\end{bmatrix}$$

The color values of the key image represent forces for the independent variable x. Since the system of third-order differential equations underwent three integration processes, the forces have increased by 3.

Consequently, for the purpose of constructing the ordinary differential equation system that we will derive three times, we increase the color values of the key image by 3 and make them forces for the independent variable x, which we will incorporate into the encrypted image **SCRAMBLE3$_{(3,6)}$** to establish an ordinary equation system that serves as a starting point for decryption to recover the original image. This system will be as follows:

System of Ordinary Equations: - SOE

$SOE_{(3,6)}$

$$= \begin{bmatrix} y_{(1,1)} = \frac{\frac{215}{129}}{\frac{130}{131}}x^{131} & y_{(1,2)} = \frac{\frac{145}{223}}{\frac{224}{225}}x^{225} & y_{(1,3)} = \frac{\frac{111}{99}}{\frac{100}{101}}x^{101} & y_{(1,4)} = \frac{\frac{145}{77}}{\frac{78}{79}}x^{79} & y_{(1,5)} = \frac{\frac{123}{115}}{\frac{116}{117}}x^{117} & y_{(1,6)} = \frac{\frac{245}{247}}{\frac{248}{249}}x^{249} \\[3em] y_{(2,1)} = \frac{\frac{221}{29}}{\frac{30}{31}}x^{31} & y_{(2,2)} = \frac{\frac{159}{223}}{\frac{224}{225}}x^{225} & y_{(2,3)} = \frac{\frac{170}{179}}{\frac{180}{181}}x^{181} & y_{(2,4)} = \frac{\frac{251}{67}}{\frac{68}{69}}x^{69} & y_{(2,5)} = \frac{\frac{154}{100}}{\frac{101}{102}}x^{102} & y_{(2,6)} = \frac{\frac{201}{110}}{\frac{111}{112}}x^{112} \\[3em] y_{(3,1)} = \frac{\frac{200}{255}}{\frac{256}{257}}x^{257} & y_{(3,2)} = \frac{\frac{233}{179}}{\frac{180}{181}}x^{181} & y_{(3,3)} = \frac{\frac{177}{245}}{\frac{246}{247}}x^{247} & y_{(3,4)} = \frac{\frac{101}{119}}{\frac{120}{121}}x^{121} & y_{(3,5)} = \frac{\frac{143}{244}}{\frac{245}{246}}x^{246} & y_{(3,6)} = \frac{\frac{125}{226}}{\frac{227}{228}}x^{228} \end{bmatrix}$$

Step One: We take the first derivative of the above ordinary equation system matrix **SOE$_{(3,6)}$** to obtain the matrix of the first-order differential equation system.

System of differential equations of the first order:-SDEFO

$SDEFO_{(3,6)}$

$$= \begin{bmatrix} y'_{(1,1)} = 131*\frac{\frac{215}{129}}{\frac{130}{131}}x^{130} & y'_{(1,2)} = 225*\frac{\frac{145}{223}}{\frac{224}{225}}x^{224} & y'_{(1,3)} = 101*\frac{\frac{111}{99}}{\frac{100}{101}}x^{100} & y'_{(1,4)} = 79*\frac{\frac{145}{77}}{\frac{78}{79}}x^{78} & y'_{(1,5)} = 117*\frac{\frac{123}{115}}{\frac{116}{117}}x^{116} & y'_{(1,6)} = 249*\frac{\frac{245}{247}}{\frac{248}{249}}x^{248} \\[3em] y'_{(2,1)} = 31*\frac{\frac{221}{29}}{\frac{30}{31}}x^{30} & y'_{(2,2)} = 225*\frac{\frac{159}{223}}{\frac{224}{225}}x^{224} & y'_{(2,3)} = 181*\frac{\frac{170}{179}}{\frac{180}{181}}x^{180} & y'_{(2,4)} = 69*\frac{\frac{251}{67}}{\frac{68}{69}}x^{68} & y'_{(2,5)} = 102*\frac{\frac{154}{100}}{\frac{101}{102}}x^{101} & y'_{(2,6)} = 112*\frac{\frac{201}{110}}{\frac{111}{112}}x^{111} \\[3em] y'_{(3,1)} = 257*\frac{\frac{200}{255}}{\frac{256}{257}}x^{256} & y'_{(3,2)} = 181*\frac{\frac{233}{179}}{\frac{180}{181}}x^{180} & y'_{(3,3)} = 247*\frac{\frac{177}{245}}{\frac{246}{247}}x^{246} & y'_{(3,4)} = 121*\frac{\frac{101}{119}}{\frac{120}{121}}x^{120} & y'_{(3,5)} = 246*\frac{\frac{143}{244}}{\frac{245}{246}}x^{245} & y'_{(3,6)} = 228*\frac{\frac{125}{226}}{\frac{227}{228}}x^{227} \end{bmatrix}$$

$SDEFO_{(3,6)}$

$$= \begin{bmatrix} y'_{(1,1)} = \frac{\frac{215}{129}}{130}x^{130} & y'_{(1,2)} = \frac{\frac{145}{223}}{224}x^{224} & y'_{(1,3)} = \frac{\frac{111}{99}}{100}x^{100} & y'_{(1,4)} = \frac{\frac{145}{77}}{78}x^{78} & y'_{(1,5)} = \frac{\frac{123}{115}}{116}x^{116} & y'_{(1,6)} = \frac{\frac{245}{247}}{248}x^{248} \\[3em] y'_{(2,1)} = \frac{\frac{221}{29}}{30}x^{30} & y'_{(2,2)} = \frac{\frac{159}{223}}{224}x^{224} & y'_{(2,3)} = \frac{\frac{170}{179}}{180}x^{180} & y'_{(2,4)} = \frac{\frac{251}{67}}{68}x^{68} & y'_{(2,5)} = \frac{\frac{154}{100}}{101}x^{101} & y'_{(2,6)} = \frac{\frac{201}{110}}{111}x^{111} \\[3em] y'_{(3,1)} = \frac{\frac{200}{255}}{256}x^{256} & y'_{(3,2)} = \frac{\frac{233}{179}}{180}x^{180} & y'_{(3,3)} = \frac{\frac{177}{245}}{246}x^{246} & y'_{(3,4)} = \frac{\frac{101}{119}}{120}x^{120} & y'_{(3,5)} = \frac{\frac{143}{244}}{245}x^{245} & y'_{(3,6)} = \frac{\frac{125}{226}}{227}x^{227} \end{bmatrix}$$

Step Two: We take the second derivative of the above ordinary equation system matrix **SOE$_{(3,6)}$** to obtain the matrix of the second-order differential equation system.

System of differential equations of the second order:-SDESO

$SDESO_{(3,6)}$

$$= \begin{bmatrix} y''_{(1,1)} = 130*\frac{\frac{215}{129}}{130}x^{129} & y''_{(1,2)} = 224*\frac{\frac{145}{223}}{224}x^{223} & y''_{(1,3)} = 100*\frac{\frac{111}{99}}{100}x^{99} & y''_{(1,4)} = 78*\frac{\frac{145}{77}}{78}x^{77} & y''_{(1,5)} = 116*\frac{\frac{123}{115}}{116}x^{115} & y''_{(1,6)} = 248*\frac{\frac{245}{247}}{248}x^{247} \\[3em] y''_{(2,1)} = 30*\frac{\frac{221}{29}}{30}x^{29} & y''_{(2,2)} = 224*\frac{\frac{159}{223}}{224}x^{223} & y''_{(2,3)} = 180*\frac{\frac{170}{179}}{180}x^{179} & y''_{(2,4)} = 68*\frac{\frac{251}{67}}{68}x^{67} & y''_{(2,5)} = 101*\frac{\frac{154}{100}}{101}x^{100} & y''_{(2,6)} = 111*\frac{\frac{201}{110}}{111}x^{110} \\[3em] y''_{(3,1)} = 256*\frac{\frac{200}{255}}{256}x^{255} & y''_{(3,2)} = 180*\frac{\frac{233}{179}}{180}x^{179} & y''_{(3,3)} = 246*\frac{\frac{177}{245}}{246}x^{245} & y''_{(3,4)} = 120*\frac{\frac{101}{119}}{120}x^{119} & y''_{(3,5)} = 245*\frac{\frac{143}{244}}{245}x^{244} & y''_{(3,6)} = 227*\frac{\frac{125}{226}}{227}x^{226} \end{bmatrix}$$

$$SDESO_{(3,6)}$$

$$=\begin{bmatrix}
y''_{(1,1)}=\dfrac{215}{129}x^{129} & y''_{(1,2)}=\dfrac{145}{223}x^{223} & y''_{(1,3)}=\dfrac{111}{99}x^{99} & y''_{(1,4)}=\dfrac{145}{77}x^{77} & y''_{(1,5)}=\dfrac{123}{115}x^{115} & y''_{(1,6)}=\dfrac{245}{247}x^{247} \\[2mm]
y''_{(2,1)}=\dfrac{221}{29}x^{29} & y''_{(2,2)}=\dfrac{159}{223}x^{223} & y''_{(2,3)}=\dfrac{170}{179}x^{179} & y''_{(2,4)}=\dfrac{251}{67}x^{67} & y''_{(2,5)}=\dfrac{154}{100}x^{100} & y''_{(2,6)}=\dfrac{201}{110}x^{110} \\[2mm]
y''_{(3,1)}=\dfrac{200}{255}x^{255} & y''_{(3,2)}=\dfrac{233}{179}x^{179} & y''_{(3,3)}=\dfrac{177}{245}x^{245} & y''_{(3,4)}=\dfrac{101}{119}x^{119} & y''_{(3,5)}=\dfrac{143}{244}x^{244} & y''_{(3,6)}=\dfrac{125}{226}x^{226}
\end{bmatrix}$$

Step Three: We take the third derivative of the above ordinary equation system matrix **SOE(3,6)** to obtain the matrix of the third-order differential equation system.

System of differential equations of the third order:-SDETO

$$SDETO_{(3,6)}$$

$$=\begin{bmatrix}
y'''_{(1,1)}=129*\dfrac{215}{129}x^{128} & y'''_{(1,2)}=223*\dfrac{145}{223}x^{222} & y'''_{(1,3)}=99*\dfrac{111}{99}x^{98} & y'''_{(1,4)}=77*\dfrac{145}{77}x^{76} & y'''_{(1,5)}=115*\dfrac{123}{115}x^{114} & y'''_{(1,6)}=247*\dfrac{245}{247}x^{246} \\[2mm]
y'''_{(2,1)}=29*\dfrac{221}{29}x^{28} & y'''_{(2,2)}=223*\dfrac{159}{223}x^{222} & y'''_{(2,3)}=179*\dfrac{170}{179}x^{178} & y'''_{(2,4)}=67*\dfrac{251}{67}x^{66} & y'''_{(2,5)}=100*\dfrac{154}{100}x^{99} & y'''_{(2,6)}=110*\dfrac{201}{110}x^{109} \\[2mm]
y'''_{(3,1)}=255*\dfrac{200}{255}x^{254} & y'''_{(3,2)}=179*\dfrac{233}{179}x^{178} & y'''_{(3,3)}=245*\dfrac{177}{245}x^{244} & y'''_{(3,4)}=119*\dfrac{101}{119}x^{118} & y'''_{(3,5)}=244*\dfrac{143}{244}x^{243} & y'''_{(3,6)}=226*\dfrac{125}{226}x^{225}
\end{bmatrix}$$

$$SDETO_{(3,6)}$$

$$=\begin{bmatrix}
y'''_{(1,1)}=215x^{128} & y'''_{(1,2)}=145x^{222} & y'''_{(1,3)}=111x^{98} & y'''_{(1,4)}=145x^{76} & y'''_{(1,5)}=123x^{114} & y'''_{(1,6)}=245x^{246} \\[2mm]
y'''_{(2,1)}=221x^{28} & y'''_{(2,2)}=159x^{222} & y'''_{(2,3)}=170x^{178} & y'''_{(2,4)}=251x^{66} & y'''_{(2,5)}=154x^{99} & y'''_{(2,6)}=201x^{109} \\[2mm]
y'''_{(3,1)}=200x^{254} & y'''_{(3,2)}=233x^{178} & y'''_{(3,3)}=177x^{244} & y'''_{(3,4)}=101x^{118} & y'''_{(3,5)}=143x^{243} & y'''_{(3,6)}=125x^{225}
\end{bmatrix}$$

From the third-order differential equation system **SDETO(3,6)** we extract the matrix associated with the independent variable x coefficients in all the differential equations of the system. Let this matrix be as follows: The image after decryption (IMAD):-

$$IMAD_{(3,6)}=\begin{bmatrix}215 & 145 & 111 & 145 & 123 & 245 \\ 221 & 159 & 170 & 251 & 154 & 201 \\ 200 & 233 & 177 & 101 & 143 & 125\end{bmatrix}$$

We observe that the color values of the image after decryption ($IMAD_{(3,6)}$) match the color values of the original image before encryption:

$$\text{The origon image befor encryption } A_{(3,6)}=\begin{bmatrix}215 & 145 & 111 & 145 & 123 & 245 \\ 221 & 159 & 170 & 251 & 154 & 201 \\ 200 & 233 & 177 & 101 & 143 & 125\end{bmatrix}$$

This result indicates the quality and accuracy of the algorithm, as well as its error-free nature.

2. Experimental results and analysis

This algorithm was implemented using MATLAB software [25], and we applied the process to five images: Suspension Bridge, Floating Bridge, Child, Lena, and Baboon. To further clarify the workflow steps, we provide below the complete results for each stage of integration in the differential equations.

Table 1.1:part one: Comprehensive breakdown of algorithm implementation on five images (Baboon, Child, Suspension Bridge, Floating Bridge, Lena) including all data and resulting readings from the algorithm execution.
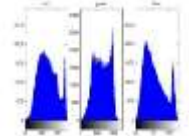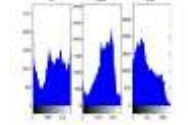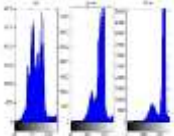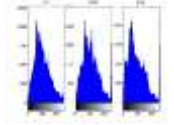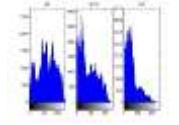
Image Name	Baboon	Child	Suspension bridge	floating bridge	Lena
Origin Image					
Histogram of origin image					
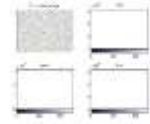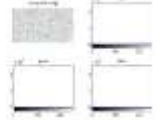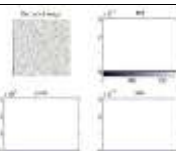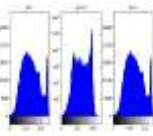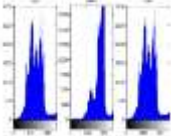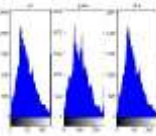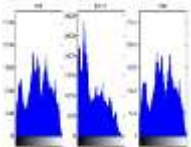
Image Name	Baboon	Child	Suspension bridge	floating bridge	Lena
Image key					
The encrypted image after the first integration					
The encrypted image after the second integration					
The encrypted image after the third integration					
Histogram of encryption image					

Table 1.2:part two: Comprehensive breakdown of algorithm implementation on five images (Baboon, Child, Suspension Bridge, Floating Bridge, Lena) including all data and resulting readings from the algorithm execution.

Image Name	Baboon	Child	Suspension bridge	floating bridge	Lena
Image after decryption					
Histogram of Image after decryption					
Encryption	1.0450	1.1540	0.8430	0.8890	1.0450

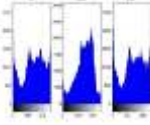| time/s					
Decryption time/s	1.6690	1.9040	1.4670	1.4980	1.7010
Mean error	0	0	0	0	0
MSE	0	0	0	0	0
PSNR	Inf	Inf	Inf	Inf	Inf
Entropy before encryption EBE	0.0030	0.0600	1.6775e-004	0.0074	0.1416
Entropy after decryption EAD	0.0030	0.0600	1.6775e-004	0.0074	0.1416
Entropy for encryption image EEI	0.0292	0.0286	0.0284	0.0271	0.0307
Standard deviation before encryption SDBE	56.1909	67.8624	46.7713	55.4479	63.8309
Standard deviation after decryption SDAD	56.1909	67.8624	46.7713	55.4479	63.8309
Standard deviation for encryption image SDEI	263.9176	293.1406	235.9069	279.7039	276.1800
Correlation coefficient between origin and image after decryption CCOAD	1	1	1	1	1
Correlation coefficient between origin and encryption image CCOE	0.0020	0.0063	-0.0067	0.0032	0.0050
NPCR	99.9999	99.9916	100	100	99.9921
UACI	33.4312	33.0764	33.3436	33.8822	33.2641
Dimension of image	512 512 3	448 600 3	361 600 3	361 600 3	512 512 3

For the analysis of global standards accuracy pre-encryption and post-decryption across various images such as Baboon, MK-image, Lena, Child, Suspension Bridge, and Floating Bridge, we ensured that Figure 1 is comprehensive with all information and readings related to international accuracy standards, eliminating the need for excessive tables and figures. The results in Figure 1 clearly show the algorithm's precision and highly great readings, especially when compared to competing methods. This will become clearer later in the comparison tables we created with past works, whether by myself as a researcher or other researchers.

Table 1 describes the differences in encryption and decryption times between our proposed method and existing techniques, including: 11

• MIE (mirror-like image encryption) [20].

• Visual Cryptography (VC).

• MK-1-4 (Mohammed al-Kufi levels 1-4). • MK-5. • MKA-6. • MKHAH-7. • MK-8. • MK-9. • MK-10. • MK-11. • MK-12. • MK-13. • MK-14 • MK-15.

Table 2 below compares two criteria (MSE and PSNR) between this algorithm and other algorithms.

Table 2. The comparison between the new approach and the previous algorithms for 5 photos (Lena, Baboon, Child, Suspension bridge, and Floating bridge).

Algorithm	Encryption time (Second)					Decryption Time (Second)				
	Image					Image				
	Lena	Baboon	Child	Suspension bridge	Floating bridge	Lena	Baboon	Child	Suspension bridge	Floating bridge
MIE	5	9.23	***	***	***	5.16	9.23	***	***	***
VC	4.56	8.35	***	***	***	****	****	***	***	***
MK-1[32]	2.224	2.287	2.126	1.67	1.535	3.11	3.166	2.716	1.94	1.936
MK-2[32]	5.368	5.508	4.882	3.384	3.318	6.013	6.104	5.429	3.734	3.696
MK-3[32]	1.456	1.459	1.425	1.066	1.073	2.138	2.159	1.995	1.434	1.445
MK-4[32]	5.54	5.567	5.115	3.532	3.574	6.265	6.382	5.818	3.871	3.895
MK-5[33]	2.522	2.338	***	***	***	2.924	3.104	***	***	***
MKA-6[34]	7.95	8.24	***	***	***	2.13	2.07	***	***	***
MKHAH-7[35]	3.53	3.45	***	***	***	3.57	3.3	***	***	***
MK-8[36]	1.799	1.898	***	***	***	0.73	0.74	***	***	***
MK-9[37]	3.35	3.46	***	***	***	3.57	3.43	***	***	***
MK-10[38]	0.5650	0.5580	***	***	***	0.6090	0.5970	***	***	***
MK-11[39]	1.349	1.3470	0.9680	0.8360	0.6910	14.0740	13.9530	13.7530	11.3280	11.1270
Our algorithm MK-16	1.0450	1.0450	1.1540	0.8430	0.8890	1.7010	1.6690	1.9040	1.4670	1.4980

Table 3.1: The part one: compares the results of the global accuracy standards (MSE and PSNR) to other image processing studies in general.

Algorithm	MSE					PSNR				
	Image					Image				
	Lena	Baboon	Child	Suspension bridge	Floating bridge	Lena	Baboon	Child	Suspension bridge	Floating bridge
SKM [10] JPEG	****	****	***	***	***	21.2	****	***	***	***
SKM [10] BPP	****	****	***	***	***	22.7	****	***	***	***
NKP [27]	****	****	***	***	***	8.67	9.076	***	***	***
DSA [28]	3.81 e-6	****	***	***	***	54.18	****	***	***	***

Table 3.2: part two: compares the results of the global accuracy standards (MSE and PSNR) to other image processing studies in general.

Algorithm	MSE					PSNR				
	Image					Image				
	Lena	Baboon	Child	Suspension bridge	Floating bridge	Lena	Baboon	Child	Suspension bridge	Floating bridge
TTV [29]	0.078	****	***	***	***	29.6041	****	***	***	***
AZA [30]	****	0.132977	***	***	***	****	56.893054	***	***	***
NDD [31]	0.0012	****	***	***	***	77.4586	****	***	***	***
MK-1 [32]	9.9137e-26	7.9003e-26	1.7071e-25	2.6112e-24	1.126e-25	125.0188	125.5118	123.8387	117.9158	124.7424
MK-2 [32]	9.9137e-26	7.9003e-26	1.7071e-25	2.6112e-24	1.126e-25	125.0188	125.5118	123.8387	117.9158	124.7424
MK-3 [32]	7.3078e-27	8.9787e-27	2.5571e-26	2.2543e-25	2.1675e-26	130.6811	130.2339	127.9612	123.235	128.3202
MK-4 [32]	9.9137e-26	7.9003e-26	1.7071e-25	2.6112e-24	1.126e-25	125.0188	125.5118	123.8387	117.9158	124.7424
MK-5 [33]	****	****	***	***	***	140.4432	143.2098	***	***	***
MKA-6 [34]	0	0	***	***	***	Inf	Inf	***	***	***
MKHAH-7 [35]	7.8839e-30	****	***	***	***	145.5163	****	***	***	***
MK-8 [36]	5.0193e-20	4.4692e-21	***	***	***	144.6276	149.8797	***	***	***
MK-9 [37]	1.9491e-006	3.8846e-006	***	***	***	28.5598	27.1084	***	***	***
MK-10	1.253	1.418	***	***	***	172.64	177.371	***	***	***

Algorithm	MSE					PSNR				
	Image					Image				
	Lena	Baboon	Child	Suspension bridge	Floating bridge	Lena	Baboon	Child	Suspension bridge	Floating bridge
[38]	2e-25	4e-26				07	9			
MK-11 [39]	2.9489e-23	2.3282e-22	6.4074e-23	3.6006e-23	2.7508e-23	160.7825	156.2957	159.0974	160.3490	160.9335
MK-12-15 [40]	0	0	0	0	0	inf	Inf	Inf	Inf	inf
Our algorithm MK-16	0	0	0	0	0	inf	Inf	Inf	Inf	inf

(∗∗∗) In tables (1 & 2) means that the address is not calculated

Conclusions

From the above figure and tables, we can conclude that our algorithm " Image encryption algorithm using differential equations" represents a significant breakthrough in encryption algorithms, as the resulting data error is zero. This makes it suitable for application in various fields and gives it the strengths listed below:

- The algorithm is applicable in medical fields.
- The algorithm is applicable in military and national security contexts.
- The algorithm is suitable for text encryption in all languages.
- The algorithm is highly resistant to intrusion attempts and code-breaking by attackers.
- Encryption and decryption times are very short compared to previous algorithms.
- The clear relationship between the original image and the image after decryption, with the latter having a maximum value of 1, indicates a high and absolute degree of correspondence between the two images. This demonstrates that no data is lost during the encryption and decryption process.

References

[1] Ahmed, F., Rehman, M. U., Ahmad, J., Khan, M. S., Boulila, W., Srivastava, G., & Buchanan, W. J. "A DNA based colour image encryption scheme using a convolutional autoencoder." ACM Transactions on Multimedia Computing, Communications and Applications, vol. 19, no. 3s, pp. 1-21, 2023.

[2] Zheng, B., Qiu, Z., & Yang, J. "A Novel Fingerprint Encryption Based on Image and Feature Mosaic." Tehnički vjesnik, vol. 29, no. 6, pp. 1914-1922, 2022.

[3] Yuan, Q., Ge, Q., Chen, L., Zhang, Y., Yang, Y., Cao, X., & Wang, Z. "Recent advanced applications of metasurfaces in multi-dimensions." Nanophotonics, (0), 2023.

[4] Zank, M. "Integral representations and quadrature schemes for the modified Hilbert transformation." Computational Methods in Applied Mathematics, vol. 23, no. 2, pp. 473-489, 2023.

[5] Zhang, B., & Liu, L. "Chaos-Based Image Encryption: Review, Application, and Challenges." Mathematics, vol. 11, no. 11, p. 2585, 2023.

[6] Zhang, F., Li, F., & Zhang, W. "Differential-Linear Cryptanalsis on SIMECK32/64 and SIMON32/64." Journal of Physics: Conference Series, vol. 2504, no. 1, p. 012068, 2023.

[7] Abdullah, R. M. (2024). A deep learning-based framework for efficient and accurate 3D real-scene reconstruction. *International Journal of Information Technology*, *16*(7), 4605-4609.

[8] Lu, X., Wang, Z., Zhao, C., Zhan, Q., & Cai, Y. "Four-dimensional experimental characterization of partially coherent light using incoherent modal decomposition." Nanophotonics, (0), 2023.

[9] Maniyath, S. R., & Thanikaiselvan, V. "A novel efficient multiple encryption algorithm for real time images." International Journal of Electrical and Computer Engineering (IJECE), vol. 10, no. 2, pp. 1327-1336, 2020.

[10] Nawaz, Y., Abodayeh, K., Arif, M. S., & Ashraf, M. U. "A third-order two-step numerical scheme for heat and mass transfer of chemically reactive radiative MHD power-law fluid." Advances in Mechanical Engineering, vol. 13, no. 10, p. 16878140211054983, 2021.

[11] Quinn, D. M., Kane, T. J., Greenberg, M., & Thal, D. "Effects of a video-based teacher observation program on the de-privatization of instruction: Evidence from a randomized experiment." Educational administration quarterly, vol. 54, no. 4, pp. 529-558, 2018.

[12] Sha, Y., Bu, F., Jahanshahi, H., & Wang, L. "A chaos-based image encryption scheme using the hamming distance and DNA sequence operation." Frontiers in Physics, vol. 10, p. 911156, 2022.

[13] Grassi, A., Gugiatti, G., Lutz, W., & Petracci, A. "Reflexive polygons and rational elliptic surfaces." arxiv preprint arxiv:2302.05751, 2023.

[14] Hutaihit, M. A., Hammed, H. M., & Shauchuk, O. (2022). Identification of Lines Based on Form Factor and Geometrical Descriptors. *International Journal of Integrated Engineering*, *14*(6), 265-274.

[15] Bazighifan, O., Mofarreh, F., & Nonlaopon, K. "On the qualitative behavior of third-order differential equations with a neutral term." Symmetry, vol. 13, no. 7, p. 1287, 2021.

[16] Cabada, A., & Dimitrov, N. D. "Third-order differential equations with three-point boundary conditions." Open Mathematics, vol. 19, no. 1, pp. 11-31, 2021.

[17] Kim, P. H., Ryu, K. W., & Jung, K. H. "Reversible data hiding scheme based on pixel-value differencing in dual images." International Journal of Distributed Sensor Networks, vol. 16, no. 7, p. 1550147720911006, 2020.

[18] Taie, R. O., & Bakhit, D. A. "Some New Results on the Uniform Asymptotic Stability for Volterra Integro-differential Equations with Delays." Mediterranean Journal of Mathematics, vol. 20, no. 5, pp. 280, 2023.

[19] Avila, J. C., Frías-Armenta, M. E., & López-González, E. "Generalized Cauchy–Riemann equations in non-identity bases with application to the algebrizability of vector fields." Forum Mathematicum (No. 0), De Gruyter, March 2023.

[20] Bohner, M., Domoshnitsky, A., Padhi, S., & Srivastava, S. N. "Vallée-Poussin theorem for equations with Caputo fractional derivative." Mathematica Slovaca, vol. 73, no. 3, pp. 713-728, 2023.

[21] Cai, Z., Li, B., Bai, Z., Liu, D., Yang, K., Liu, B., & Liao, C. "Encrypted optical fiber tag based on encoded fiber Bragg grating array." International Journal of Extreme Manufacturing, vol. 5, no. 3, p. 035502, 2023.

[22] Cauchy, A. "Démonstration du omplet omplet de Fermat sur les nombres polygones." In Oeuvres ompletes d'Augustin Cauchy, Vol. VI (II Série). Paris: Gauthier-Villars, pp. 320-353, 1905.

[23] Deb, S., Jafari, H., Das, A., & Parvaneh, V. "New fixed-point theorems via measure of noncompactness and its application on fractional integral equation involving an operator with iterative relations." Journal of Inequalities and Applications, vol. 2023, no. 1, pp. 1-18, 2023.

[24] Eiter, T., Hopf, K., & Lasarzik, R. "Weak-strong uniqueness and energy-variational solutions for a class of viscoelastoplastic fluid models." Advances in Nonlinear Analysis, vol. 12, no. 1, p. 20220274, 2022.

[25] Jiang, D., Yuan, Z., Li, W. x., & Lu, L. L. "Real-time chaotic video encryption based on multithreaded parallel confusion and diffusion." arxiv preprint arxiv:2302.07411, 2023.

[26] Liebsch, M., Russenschuck, S., & Kurz, S. "BEM-based magnetic field reconstruction by ensemble Kálmán filtering." Computational Methods in Applied Mathematics, vol. 23, no. 2, pp. 405-424, 2023.

[27] MATLAB-professional License- R2016a (9.0.0.341360)-24-bit (win 64)- february 11, 2016- License Number: 123456.

[28] Shaimaa A., Khalid F. A., Mohamed M. F. 2011. Securing Image Transmission Using In- Compression Encryption Technique. International Journal of Computer Science and Security, (IJCSS), 4(5): 466-48

[29] Narendra K P. 2012. Image encryption using chaotic logistic map, ELSEVIER. 24(9).: 926-934

[30] Deepak A., Sandeep K., Anantdeep A. 2010. An Efficient Watermarking Algorithm To Improve Payload And Robustness Without Affecting Image Perceptual Quality, Journal of Computing.2(4). 105-109

[31] Trinadh T., Venkata N. 2012. A Novel PSNR-B Approach for Evaluating the Quality of De-blocked Images. IOSR Journal of Computer Engineering. 4(5).: 40-49

[32] Amira B. S., Zahraa M. T. Ahmed S. N. 2010. An Investigation for Steganography using Different Color System. Rafidain Journal of Computer Science and Mathematics for the year. Proceedings of the Third Scientific Conference on Technology of information.

Naitik P K., Dipesh G. K., Dharmesh N.K. Performance Evaluation of LSB Based Steganography For Optimization of PSNR and MSE. Journal of Information, Knowledge and Research in Electronics and Communication Engineering. ISSN: 0975 – 6779| NOV 12 TO OCT 13 | VOLUME – 02, ISSUE - 02 :Pages 505-509 http://www.ejournal.aessangli.in/ASEEJournals/EC98.pdf

[33] Mohammed Abdul- Hameed Jassim Al- Kufi; Image Encryption with Singular Values Decomposition Aided; Msc. Thesis to Faculty of Computer Science & Mathematics- University of Kufa- 2014

[34] Nidhal K. El Abbadi, Adil Mohamad and Mohammed Abdul-Hameed, IMAGE ENCRYPTION BASED ON SINGULAR VALUE DECOMPOSITION, Journal of Computer Science, Vol 10 (7): 1222-1230, 2014

[35] Adil AL-Rammahi& Mohammed Al-kufi; Image Cryptography Via SVD Modular Numbers; European Journal of Scientific Research- Volume 138 No 2 - February, 2016

[36] Mohammed Abdul Hameed Jassim Al-Kufi , Hayder Raheem Hashim , Ameer Mohammed Hussein, and Hind Rustum Mohammed; An Algorithm Based on GSVD for Image Encryption. Math. Comput. Appl. 2017, 22, 28; doi: 10.3390/mca22020028 www.mdpi.com/journal/mca

[37] Mohammed Abdul Hameed Jassim Al-Kufi; An a New Algorithm Based on (General Singular Values Decomposition) and (Singular Values Decomposition) for Image Cryptography; Elixir Digital Processing 114 (2018) 49604-49609

[38] Mohammed Abdul Hameed Jassim Al-Kufi; Dheiaa Shakir Redhaa , Mujtaba Zuhair Ali IMAGE ENCRYPTION & DECRYPTION VIA (GSVD-MODULAR NUMBERS), Journal of Engineering and Applied Sciences 15-11-2018

[39] Mohammed Abdul Hameed Jassim Al Kufi; Ola N. Kadhim , Eman Saleem Razaq Simulate a first-order Bézier curve in image encoding, , Journal of Physic- 31-5-2020

[40] Mohammed Abdul Hameed Jassim Al Kufi; Image encryption with General Singular Values Decomposition via logistic function by encryption key only real number (method-2), Journal of Interdisciplinary Mathematics, 10-10-2023

[41] Mohammed Abdul Hameed Jassim Al Kufi; Hussein Abbas Al-Salihi- Data and image encryption through steganography inside an image (MKTExT-7) and (MK-12,13,14,15), International Journal of nonlinear Analysis and applications- 9-2023